



Contents lists available at ScienceDirect

Journal of Organometallic Chemistry

journal homepage: www.elsevier.com/locate/jorganchem

Biological assessment of novel bisphosphonate-containing $^{99m}\text{Tc}/\text{Re}$ -organometallic complexes

Célia Fernandes^{a,1}, Sofia Monteiro^{a,1}, Patrícia Mendes^a, Lurdes Gano^a,
Fernanda Marques^a, Sandra Casimiro^b, Luís Costa^b, João D.G. Correia^{a,*}, Isabel Santos^{a,*}

^a Centro de Ciências e Tecnologias Nucleares, Instituto Superior Técnico, Universidade de Lisboa, Estrada Nacional 10 (ao km 139,7), 2695-066 Bobadela LRS, Portugal

^b Instituto de Medicina Molecular, Faculdade de Medicina, Universidade de Lisboa, Lisboa, Portugal

ARTICLE INFO

Article history:

Received 4 October 2013

Received in revised form

16 October 2013

Accepted 21 October 2013

Dedicated to Prof. M.J. Calhorda on the occasion of her 65th birthday.

Keywords:

Bisphosphonates

Bone

Biodistribution

Cell assays

Rhenium

Technetium-99m

ABSTRACT

Bone-seeking radiopharmaceuticals such as radiolabeled bisphosphonates (BPs) bind to bone matrix in areas of increased bone turnover, characteristic of metastazition sites, delivering selectively γ radiation or β^- particles for bone imaging or bone-pain palliation, respectively. Recent preclinical studies suggest that nitrogen-containing BPs may have also a direct anti-tumor activity. We have recently introduced a set of ^{99m}Tc -organometallic complexes that allow the simultaneous delivery of γ radiation and BPs to bone tissue. Aimed at finding complexes of the same family with improved bone-seeking properties and adequate tumor cell uptake profile, we have synthesized novel complexes of the type *fac*- $[\text{M}(\text{CO})_3(\text{k}^3\text{-L})]^+$ ($\text{M} = ^{99m}\text{Tc}/\text{Re}$, **Tc3/Re3–Tc5/Re5**) stabilized by bifunctional chelators with different molecular weight, overall charge, (lipo)hydrophilic nature and different positions of BP attachment. Biodistribution studies in normal mice have shown that **Tc3**, where the BP unit (alendronate) is at position 4 of the pyrazolyl ring, presents the most favorable pharmacokinetic profile with fast blood clearance, high bone uptake ($17.1 \pm 3.6\%$ I.A./g at 1 h p.i.), and higher bone-to-blood and bone-to-muscle ratios than the gold standard ^{99m}Tc -MDP. Cellular uptake studies in the MDAMB231 metastatic breast cancer cells showed a maximal uptake of 4–6% at 6 h incubation for all complexes. Interestingly, cell fragmentation studies have shown that **Tc3** presents the highest accumulation in the cytosol (35%). The promising biological profile of the BP-containing complex **Tc3** encourages further research towards evaluation of ^{188}Re congeners for potential therapeutic applications.

© 2013 Elsevier B.V. All rights reserved.

1. Introduction

Many patients with cancer develop symptomatic skeletal metastases at an advanced stage of their disease. This situation is often complicated by pain and present considerable morbidity and mortality. Besides analgesics, treatment options include external beam radiotherapy, bisphosphonates, chemotherapy, surgery and bone-seeking radiopharmaceuticals [1,2]. The latter binds to the bone matrix in areas of increased bone turnover characteristic of metastazition sites. The result is the selective delivery of beta particles to areas of amplified osteoblastic activity, and targeting simultaneously multiple metastases, both symptomatic and asymptomatic foci, leading to a pain therapeutic/palliative effect.

Using the match pair $^{186/188}\text{Re}$ (β^- -emitters) and ^{99m}Tc (γ -emitter), skeletal systemic radiotherapy and radiodiagnostics, respectively, is possible [3,4]. This systemic form of radiotherapy is simple to administer and complements other treatment options, although it has not been possible so far to combine with chemotherapy or bisphosphonates [2]. In vitro analysis of the anti-tumoral effect of bisphosphonates on human breast cancer cell lines indicated that they have direct anti-tumor effects and also inhibit breast and prostate carcinoma tumor cell invasion and cell adhesion to bone [5–10]. Zoledronic acid combined with external radiation caused a decrease in cell viability and, for the first time, synergistic cytotoxic effect was confirmed by isobologram analysis [11]. Moreover, there is recent preclinical evidence that nitrogen-containing bisphosphonates display a certain degree of anti-tumor activity, which has been attributed to an indirect mechanism (osteolysis inhibition/decrease in growth factors released from the bone matrix). Recently, preclinical studies have also indicated that bisphosphonates, such as zoledronic acid, may have also a direct anti-tumor

* Corresponding authors. Tel.: +351 21 994 62 01.

E-mail addresses: jgalamba@itn.pt, jgalcorr@gmail.com (J.D.G. Correia), isantos@itn.pt (I. Santos).

¹ These authors contributed equally to the manuscript.

activity [5,6]. Zoledronic acid-mediated apoptosis is associated with cytochrome *c* release and consequent caspase activation, a process that may be initiated by inhibition of key enzymes in mevalonate pathway leading to impaired prenylation of intracellular proteins including Ras and RhoA, with subsequent inhibition of chemotaxis induced by SDF-1, a chemokine significantly involved in cancer metastasis to bone [7,10].

Taking these results into consideration, we hypothesized that the combination of a bisphosphonate unit and a beta emitter radionuclide (^{188}Re or ^{186}Re) in the same molecular multi-functional compound, would lead to a synergistic effect in pain therapy and/or cancer progression, compared to the conventional sequential treatment. Following our previous studies, which aimed at the design of novel $^{99\text{m}}\text{Tc}$ (I)-labeled bisphosphonates with improved bone-seeking properties, we have synthesized and biologically evaluated the complexes **Tc1** and **Tc2** (Fig. 1), which display high bone uptake, comparable to the gold standard $^{99\text{m}}\text{Tc}$ -MDP. Both complexes allowed the simultaneous delivery of γ radiation and bisphosphonates to bone tissue in a high specific and selective way. Profiting from this fact, herein we extended the family of M(I)-labeled bisphosphonates previously reported in order to include novel complexes (**Tc3/Re3–Tc5/Re5**) with various molecular weights, overall charge, (lipo)hydrophilicities and different positions of BP attachment (Fig. 1). We will also present the biodistribution profile of the $^{99\text{m}}\text{Tc}$ (I) complexes as well as the cellular uptake studies in a metastatic breast cancer cell model in order to evaluate their potential both as bone-seeking agents and cytotoxic agents.

2. Results and discussion

2.1. Synthesis and characterization of L1–L3

The multistep procedure for the synthesis of the bifunctional ligands **L1–L3** with a pendant bisphosphonate unit is displayed in Scheme 1. Activation of the free carboxylic acid group of the pyrazolyl ring in precursor **I** with TFF/EDC, followed by reaction with alendronate afforded an intermediate, which after purification by Sep-Pak C18 cartridge and final Boc deprotection gave **L1**.

The symmetric bifunctional ligand **L2** was obtained in moderate yield (60%) by *N*-alkylation of the primary amine in alendronate with excess of precursor **IV** under basic conditions. Aiming to improve the reaction yield we have varied the reaction conditions, namely time, temperature and stoichiometric ratio. However, in all

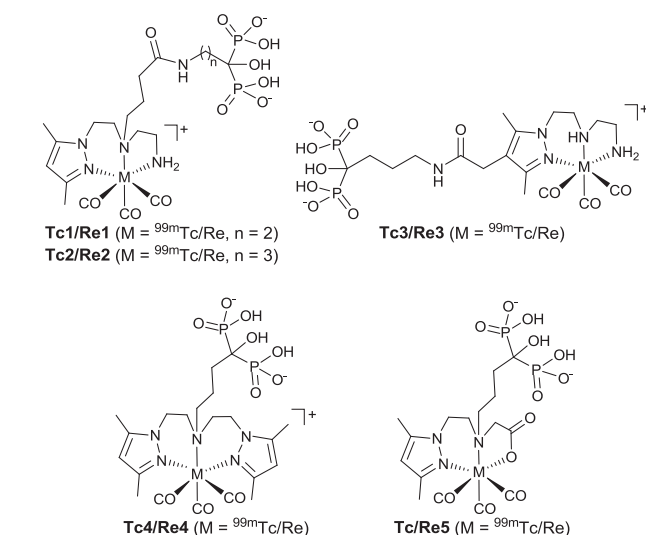


Fig. 1. $\text{M}(\text{CO})_3$ -complexes containing pendant bisphosphonate units ($M = ^{99\text{m}}\text{Tc}$, Re).

cases the *N*-monoalkylated product **V** was also obtained. After isolation, this compound has been used as starting material for the synthesis of **L3** after alkylation with bromoacetic acid.

All bifunctional ligands were fully characterized by the usual analytical techniques in chemistry, including multinuclear NMR spectroscopy (^1H , ^{13}C and ^{31}P), mass spectrometry (ESI–MS), IR spectroscopy and RP–HPLC. Brought together, the analytical data confirm the assigned structure.

2.2. Synthesis and characterization of Re3–Re5

The organometallic complexes **Re3–Re5** were synthesized and characterized as non-radioactive surrogates of the corresponding $^{99\text{m}}\text{Tc}$ congeners aiming to identify their molecular structure by means of HPLC comparison. The complexes **Re3–Re5** were prepared by ligand exchange reaction of the precursor $[\text{Re}(\text{CO})_3(\text{H}_2\text{O})_3]\text{Br}$ with **L1–L3**, respectively (Fig. 1). Complex **Re3** was synthesized in refluxing water overnight after pH adjustment (pH 6–7), whereas the synthesis of **Re4** and **Re5** was run in a NMR tube at 80 °C using D_2O as reaction solvent and DCl or KOD for pH adjustment (**Re4**, pH 7; **Re5**, pH 4). In the latter case, progression of the reactions was monitored by ^1H and ^{31}P NMR spectroscopy. All resulting complexes were purified by solid-phase extraction using Sep-Pack C18 cartridges, following the procedure described in the experimental part.

The complexes were fully characterized by infrared and multinuclear (^1H , ^{13}C and ^{31}P) magnetic resonance spectroscopy, mass spectrometry (ESI–MS) and RP–HPLC. Brought together, the data obtained were consistent with a $\kappa^3\text{-N}_3$ or $\kappa^3\text{-N}_2\text{O}$ coordination mode for the pyrazolyl-containing chelator, as found in other similar $\text{Re}(\text{I})$ complexes already described [12–14].

The IR data indicated a facial arrangement of the carbonyl groups in the complexes, with very strong ν (CO) stretching bands in the range 2033–1820 cm^{-1} , as previously found for related complexes with the moiety *fac*- $\text{Re}(\text{CO})_3$ [15]. Moreover, the IR spectrum of **Re5** present a very strong band at 1617 cm^{-1} due to the ν (C=O) stretching vibration indicating that the oxygen from the carboxylic acid participates in the coordination sphere ($\Delta\nu$ (C=O) = 68 cm^{-1} relatively to the free ligand).

The ^1H NMR spectra of **Re3–Re5** displayed the characteristic sharp singlet peaks assigned to methyl groups of the pyrazolyl ring (**Re3**, δ 2.14/2.25; **Re4**, δ 2.05/2.14, **Re5** δ 2.13/2.29). Unlike **Re3**, the spectra of **Re4** and **Re5** display also sharp singlet peaks assigned to H(4) (**Re4**, δ 5.95; **Re5**, δ 5.99) of the azolyl ring. Owing to the tridentate coordination mode of **L1–L3** the methylenic protons of the ligand backbone become diastereotopic displaying chemical shifts and splitting pattern comparable to those found for other previously reported complexes of the same type [12–14]. Moreover, unlike **Re4** and **Re5**, the spectrum of **Re3** presents also resonances assigned, respectively to the tertiary amine (δ 6.5) and to the NH_2 protons (δ 4.97 and δ 3.64) which became diastereotopic upon coordination of the amine group to the metal center.

The ^{13}C NMR spectra presented resonances for all the carbon nuclei expected for **Re3** and **Re4**.

The ^{31}P NMR spectra of all complexes present only one singlet at δ 19.0 (**Re3**), δ 23.0 (**Re4**) and δ 18.3 (**Re5**). No significant shift of these resonances relatively to the ones of the respective free ligands (**L1**, δ 19.6; **L2**, δ 18.7; **L3**, δ 18.7) was found, which is a clear indication that the terminal bisphosphonic acid group is not involved in the coordination to the metal [16].

2.3. Radiosynthesis of complexes of the type *fac*- $[\text{Re}(\text{CO})_3(\text{k}^3\text{-L})]$ (**Tc3**, L = **L1**; **Tc4**, L = **L2**; **Tc5**, L = **L3**)

The complexes **Tc3–Tc5** were prepared in high yield (>95%) and radiochemical purity (>95%) by reaction of the radioactive

than the latter, its ionic interaction with the Ca^{2+} cations of the HA matrix is favored, leading to stronger binding.

Brought together, the results of the HA adsorption studies prompted us to assess the *in vivo* properties of all radioactive complexes.

3. Biodistribution studies

Biodistribution studies of **Tc3**–**Tc5** were carried out in normal Balb/c mice at 1 h, 4 h and 6.5 h post intravenous injection (p.i.) to assess their pharmacokinetic profile, bone affinity and *in vivo* stability. Data from these studies are summarized for the most relevant organs in Table 1. For comparison, we have also evaluated, in the same animal model, the tissue distribution profile of $^{99\text{m}}\text{Tc}$ -MDP. The tissues uptake was calculated and expressed as a percentage of the injected activity per gram of tissue. The whole-body radioactivity excretion was determined as a percentage of the total injected activity.

The biodistribution data have demonstrated that all complexes are cleared from blood via both the hepatic and the renal pathways with a moderate total radioactivity excretion. The most remarkable feature of all compounds is the rapid accumulation and long retention time in the bone. In spite of the similar tissue distribution trend, there are significant differences in their pharmacokinetics. Whereas **Tc3** and **Tc4** have a fast blood clearance, especially the former ($0.21 \pm 0.05\%$ I.A./g blood at 1 h p.i.), **Tc5** presents the slowest clearance ($6.4 \pm 2.1\%$ I.A./g, $1.11 \pm 0.06\%$ I.A./g and $0.62 \pm 0.04\%$ I.A./g, at 1, 4 and 6.5 h respectively). The amount of activity eliminated by either the hepatobiliary or the urinary routes is also significantly different among the compounds. **Tc4** shows the highest accumulation of activity in the hepatobiliary tract and consequently the slowest total excretion. This finding is consistent with the less hydrophilic character of this complex.

Complexes **Tc3** and **Tc4** present a high bone uptake ($17.1 \pm 3.6\%$ I.A./g and $17.7 \pm 3.0\%$ I.A./g, respectively, at 1 h p.i.), similar to that previously found for **Tc2**, which bears the same BP unit ($17.3 \pm 6.1\%$ I.D./g), and to that of $^{99\text{m}}\text{Tc}$ -MDP ($17.1 \pm 2.4\%$ I.D./g) [15]. The lowest radioactivity accumulation in the bone was found for **Tc5**. All the compounds have a long residence in the bone up to 6.5 h, however, contrasting with $^{99\text{m}}\text{Tc}$ -MDP, a slight washout was observed at later time points. The high bone uptake of **Tc3** associated to the fast clearance from blood stream and soft tissues like muscle resulted in a significantly higher bone-to-blood and bone-to-muscle radioactivity ratio (Table 1). Moreover, this complex shows also a significantly higher bone-to-blood and bone-to-muscle ratios than **Tc2** and $^{99\text{m}}\text{Tc}$ -MDP, as displayed in Fig. 3. Furthermore, **Tc3** has the fastest overall excretion rate among all complexes ($59.5 \pm 4.0\%$ I.A., $67.3 \pm 4.1\%$ I.A. and $66.4 \pm 2.7\%$ I.A., at 1, 4 and 6.5 h respectively), which is slightly slower than that previously described for **Tc2** ($66.8 \pm 7.6\%$ I.A., $77.2 \pm 0.5\%$ I.A. and $78.2 \pm 1.6\%$ I.A., at 1, 4 and 6.5 h respectively) but significantly higher than that found for $^{99\text{m}}\text{Tc}$ -MDP ($49.1 \pm 6.1\%$ I.A., $56.8 \pm 0.9\%$ I.A. and $59.7 \pm 1.7\%$ I.A., at 1, 4 and 6.5 h respectively) in the same animal model [15].

The *in vivo* stability of **Tc3**–**Tc5** was assessed by RP-HPLC analysis of blood and urine samples collected at sacrifice time. The radiochromatograms indicated that all complexes are stable and, as an illustrative example, those obtained for **Tc3** are presented in Fig. 4.

Brought together, the biodistribution studies demonstrate that all complexes are able to deliver radiation to bone in a very selective way. However, in order to elicit a cytotoxic effect, namely through inhibition of key enzymes of the mevalonate pathway, the complexes must cross the cell membrane and be retained in the cytoplasm in order to interact with the putative cytosolic

Table 1
Biodistribution of **Tc3**–**Tc5** in normal adult Balb/c mice ($n = 4$ – 5) at 1 h, 4 h and 6.5 h p.i. (% I.A./g).

Tissue	% I.A./g \pm SD																						
	Tc3			Tc4			Tc5			$^{99\text{m}}\text{Tc}$ -MDP			Tc3			Tc4			Tc5				
	1 h	4 h	6.5 h	1 h	4 h	6.5 h	1 h	4 h	6.5 h	1 h	4 h	6.5 h	1 h	4 h	6.5 h	1 h	4 h	6.5 h	1 h	4 h	6.5 h		
Blood	0.21 \pm 0.05	0.07 \pm 0.01	0.08 \pm 0.01	1.6 \pm 0.2	0.56 \pm 0.20	0.5 \pm 0.1	6.4 \pm 2.1	1.11 \pm 0.06	0.62 \pm 0.04	0.4 \pm 0.1	0.28 \pm 0.02	0.24 \pm 0.02	0.4 \pm 0.1	0.28 \pm 0.02	0.24 \pm 0.02	0.4 \pm 0.1	0.28 \pm 0.02	0.24 \pm 0.02	0.4 \pm 0.1	0.28 \pm 0.02	0.24 \pm 0.02	0.4 \pm 0.1	
Liver	4.9 \pm 0.7	4.0 \pm 0.5	3.0 \pm 0.2	10.0 \pm 1.7	5.0 \pm 1.0	4.7 \pm 0.5	6.2 \pm 1.2	2.7 \pm 0.4	1.2 \pm 0.1	3.7 \pm 1.6	3.0 \pm 0.5	2.2 \pm 0.4	3.7 \pm 1.6	3.0 \pm 0.5	2.2 \pm 0.4	3.7 \pm 1.6	3.0 \pm 0.5	2.2 \pm 0.4	3.7 \pm 1.6	3.0 \pm 0.5	2.2 \pm 0.4	3.7 \pm 1.6	
Intestine	0.49 \pm 0.07	0.3 \pm 0.2	0.32 \pm 0.02	4.8 \pm 0.5	3.9 \pm 1.4	2.2 \pm 0.5	3.2 \pm 0.4	4.5 \pm 0.7	4.7 \pm 0.7	0.24 \pm 0.04	0.6 \pm 0.1	0.2 \pm 0.1	0.24 \pm 0.04	0.6 \pm 0.1	0.2 \pm 0.1	0.24 \pm 0.04	0.6 \pm 0.1	0.2 \pm 0.1	0.24 \pm 0.04	0.6 \pm 0.1	0.2 \pm 0.1	0.24 \pm 0.04	
Kidney	1.3 \pm 0.2	1.1 \pm 0.3	0.9 \pm 0.2	5.2 \pm 0.4	3.0 \pm 0.2	1.8 \pm 1.1	3.2 \pm 0.5	1.9 \pm 0.6	1.3 \pm 0.4	2.4 \pm 0.4	2.2 \pm 0.3	1.7 \pm 0.2	2.4 \pm 0.4	2.2 \pm 0.3	1.7 \pm 0.2	2.4 \pm 0.4	2.2 \pm 0.3	1.7 \pm 0.2	2.4 \pm 0.4	2.2 \pm 0.3	1.7 \pm 0.2	2.4 \pm 0.4	
Muscle	0.4 \pm 0.1	0.3 \pm 0.1	0.04 \pm 0.03	0.66 \pm 0.06	0.5 \pm 0.1	0.04 \pm 0.02	0.5 \pm 0.2	0.36 \pm 0.04	0.09 \pm 0.02	0.5 \pm 0.1	0.4 \pm 0.1	0.5 \pm 0.1	0.5 \pm 0.1	0.4 \pm 0.1	0.5 \pm 0.1	0.5 \pm 0.1	0.4 \pm 0.1	0.5 \pm 0.1	0.5 \pm 0.1	0.4 \pm 0.1	0.5 \pm 0.1	0.5 \pm 0.1	
Bone	17.1 \pm 3.6	14.3 \pm 2.3**	9.4 \pm 1.1	17.7 \pm 3.0	13.6 \pm 3.6*	13.0 \pm 1.7	9.3 \pm 2.1***	12.1 \pm 0.7***	8.4 \pm 1.5	17.1 \pm 2.4	19.8 \pm 1.5	18.2 \pm 3.1	17.1 \pm 2.4	19.8 \pm 1.5	18.2 \pm 3.1	17.1 \pm 2.4	19.8 \pm 1.5	18.2 \pm 3.1	17.1 \pm 2.4	19.8 \pm 1.5	18.2 \pm 3.1	17.1 \pm 2.4	
Stomach	0.5 \pm 0.3	0.19 \pm 0.09	0.4 \pm 0.1	0.6 \pm 0.2	0.5 \pm 0.2	0.5 \pm 0.1	1.6 \pm 0.4	1.3 \pm 0.6	1.2 \pm 0.8	1.0 \pm 0.7	1.5 \pm 0.4	0.4 \pm 0.1	1.0 \pm 0.7	1.5 \pm 0.4	0.4 \pm 0.1	1.0 \pm 0.7	1.5 \pm 0.4	0.4 \pm 0.1	1.0 \pm 0.7	1.5 \pm 0.4	0.4 \pm 0.1	1.0 \pm 0.7	
B/B	71.4 \pm 13.1**	210 \pm 37.7***	112.8 \pm 4.6*	11.2 \pm 1.6***	24.7 \pm 1.4**	26.1 \pm 5.0**	1.5 \pm 0.3***	10.8 \pm 0.1***	13.5 \pm 2.4***	41.9 \pm 8.1	70.9 \pm 9.2	78.1 \pm 14.3	41.9 \pm 8.1	70.9 \pm 9.2	78.1 \pm 14.3	41.9 \pm 8.1	70.9 \pm 9.2	78.1 \pm 14.3	41.9 \pm 8.1	70.9 \pm 9.2	78.1 \pm 14.3	41.9 \pm 8.1	70.9 \pm 9.2
B/M	37.2 \pm 16.5	53.6 \pm 18.0*	277.5 \pm 24.9*	26.7 \pm 2.7*	30.2 \pm 9.7*	141.0 \pm 7.5***	20.7 \pm 6.9*	33.4 \pm 4.0	99.9 \pm 30.7**	31.7 \pm 4.0	47.9 \pm 13.6	40.3 \pm 7.1	31.7 \pm 4.0	47.9 \pm 13.6	40.3 \pm 7.1	31.7 \pm 4.0	47.9 \pm 13.6	40.3 \pm 7.1	31.7 \pm 4.0	47.9 \pm 13.6	40.3 \pm 7.1	31.7 \pm 4.0	47.9 \pm 13.6
Total	59.5 \pm 4.0	67.3 \pm 4.1	66.4 \pm 2.7	37.5 \pm 1.6	47.7 \pm 4.3	55.7 \pm 2.1	54.0 \pm 4.6	57.6 \pm 2.8	65.3 \pm 2.7	49.1 \pm 6.1	56.8 \pm 0.9	59.7 \pm 1.7	49.1 \pm 6.1	56.8 \pm 0.9	59.7 \pm 1.7	49.1 \pm 6.1	56.8 \pm 0.9	59.7 \pm 1.7	49.1 \pm 6.1	56.8 \pm 0.9	59.7 \pm 1.7	49.1 \pm 6.1	56.8 \pm 0.9
Excretion (% I.A.)																							

B/B – bone-to-blood radioactivity ratio.
B/M – bone-to-muscle radioactivity ratio.
 $p < 0.05$ vs MDP.

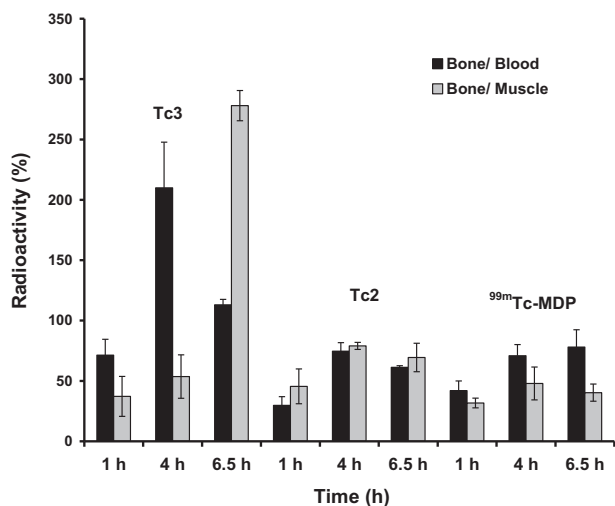


Fig. 3. Bone-to-blood and bone-to-muscle radioactivity ratios of **Tc3** in comparison with **Tc2** and ^{99m}Tc-MDP in Balb/c mice at different time points p.i.

targets. Therefore, aiming to assess this issue, we have performed cellular uptake studies in the MDAMB231 breast cancer cells. These cells were selected taking into consideration their ability to induce bone metastases. The results of the cellular uptake as a function of incubation time is presented in Fig. 5. All complexes present a very similar profile, with a maximal uptake of 4–6% at 6 h incubation, which is significantly higher than the value found for ^{99m}Tc-MDP at 6 h ($0.90 \pm 0.004\%$), under the same experimental conditions.

In order to evaluate complex cellular distribution, MDAMB231 cells were exposed to **Tc2–Tc5** during 6 h at 37 °C, and the cytosol, membrane, nucleus and cytoskeletal fractions were isolated and the radioactivity of each fraction counted. The results depicted in Fig. 6 show that all radioactive complexes accumulate preferentially at the membrane (>50%). More than 20% total activity was found in the cytosol and nucleus in particular for complexes **Tc2** (35%) and **Tc3** (44%). The latter complex **Tc3** presented the highest accumulation in the cytosol (35%).

Taking into consideration the results from biodistribution studies, cellular uptake and cellular distribution, **Tc3** appeared as the most promising radioactive bisphosphonate to be further evaluated for therapeutic purposes.

4. Conclusions

We have synthesized and characterized a set of new bisphosphonate-containing bifunctional chelators and respective

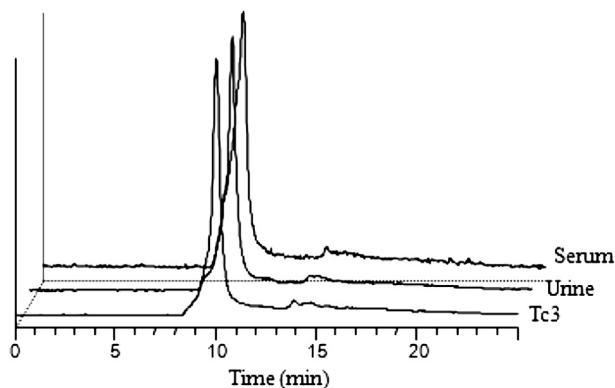


Fig. 4. RP-HPLC chromatograms (radiometric detection) of blood and urine from Balb/c mice injected with **Tc3**, at 1 h p.i.

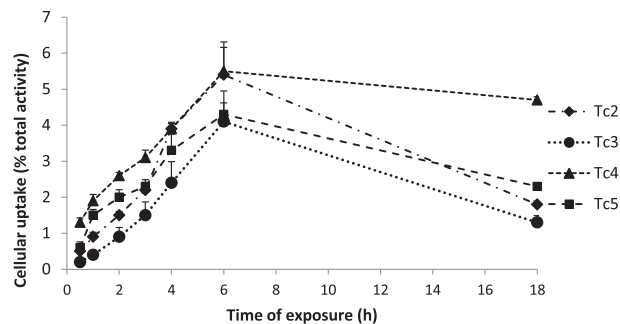


Fig. 5. Cellular uptake of **Tc2–Tc5** complexes at 37 °C in MDAMB231 breast cancer cells.

Re/^{99m}Tc tricarbonyl complexes. The ^{99m}Tc-organometallic complexes (**Tc3–Tc5**) were obtained in high yield and radiochemical purity. The biodistribution studies in normal mice demonstrated that all complexes are rapidly taken up by the bone with long residence times. Complex **Tc3** presents the most favorable pharmacokinetic profile with fast blood clearance, high bone uptake and higher bone-to-blood and bone-to-muscle ratios than the gold standard ^{99m}Tc-MDP. Among all complexes, **Tc3** shows the highest accumulation in the cytosol, an important requisite for inhibition of key enzymes in the mavelonate pathway, which is related to potential anti-tumor activity. The promising biological properties of the BP-containing complex **Tc3**, both in tumor cells and mice, encourages further research towards evaluation of its ¹⁸⁸Re congener for bone metastases therapy.

5. Experimental section

5.1. Chemistry

Unless otherwise stated, all chemicals and solvents were of reagent grade and used without purification. The compounds 2-(1-(2-(tert-butoxycarbonyl(2-(tert-butoxycarbonylamino)ethyl) amino)ethyl)-3,5-dimethyl-1H-pyrazol-4-yl)acetic acid [14], (4-Amino-1-hydroxybutylidene)bisphosphonic acid trisodium salt tetrahydrate (Alendronate, ALN) [17], 1-(2-bromoethyl)-3,5-dimethyl-1H-pyrazole [18] and tert-butyl 2-bromoethylcarbamate [19] were prepared according to published methods. The purification of the bisphosphonate-containing compounds was achieved by using Sep-Pak C18 cartridges (Waters Co., 12 cc/2 g) preconditioned according to the manufacturer's protocol and, unless otherwise stated, eluted using a H₂O–MeOH gradient. Elution of the products started with water, followed by mixtures of MeOH–

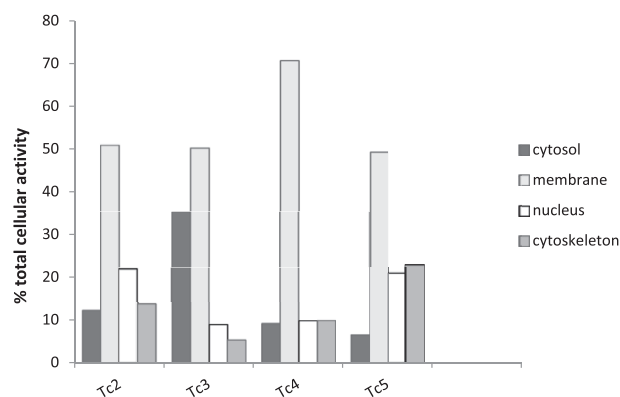


Fig. 6. Cellular distribution of **Tc2–Tc5** in MDAMB231 cells after 6 h at 37 °C.

H₂O (20–100%). The presence of bisphosphonates in the elution fractions was monitored by TLC (thin-layer chromatography) using the Dittmer's reagent as the revelator agent [20].

The ¹H, ¹³C and ³¹P NMR spectra were recorded on a Varian Unity 300 MHz spectrometer. ¹H and ¹³C chemical shifts are given in ppm and were referenced with the residual solvent resonances relative to SiMe₄ and the ³¹P chemical shifts with external 85% H₃PO₄ solution. IR spectra were recorded as KBr pellets on a Bruker, Tensor 27 spectrometer. Electrospray ionization mass spectrometry (ESI–MS) was performed at ITN on a QITMS instrument. The starting material *fac*-[Re(CO)₃(H₂O)₃]Br was synthesized by the literature method [21]. Na[^{99m}TcO₄] was eluted from a commercial ⁹⁹Mo/^{99m}Tc generator, using 0.9% saline solution. The radioactive precursor *fac*-[^{99m}Tc(CO)₃(H₂O)₃]⁺ was prepared using an Iso-LinkR[®] kit (Covidean/Malinckrodt).

Column chromatography was performed with silica gel 60 (Merck). HPLC analysis of the Re and ^{99m}Tc complexes was performed on a Perkin–Elmer LC pump 200 coupled to a LC 290 tunable UV–Vis detector and to a Berthold LB-507A radiometric detector, using an analytic Macherey–Nagel C18 reversed-phase column (Nucleosil 100–10, 250 × 4 mm) with a flow rate of 1 mL/min. HPLC solvents consisted of 0.5% CF₃COOH in H₂O (solvent A) and 0.5% CF₃COOH solution in acetonitrile (solvent B), gradient: *t* = 0–3 min, 0% eluent B; 3–3.1 min, 0–25% eluent B; 3.1–9 min, 25% eluent B; 9–9.1 min, 25–34% eluent B; 9.1–20 min, 34–100% eluent B; 20–24 min, 100% eluent B; 24–26 min, 100–0% eluent B; 26–30 min, 0% eluent B. HPLC analysis of L1–L3 was performed with solvents consisted of 0.1% CF₃COOH in H₂O (solvent A) and 0.1% CF₃COOH solution in acetonitrile (solvent B). Gradient for L1–L3 analysis: *t* = 0–5 min, 0% eluent B; 5–20 min, 5–95% eluent B; 20–20.1 min, 100% eluent B; 20.1–30 min, 100% eluent B. Gradient for L3 analysis: *t* = 0–5 min, 0% eluent B; 5–20 min, 40–60% eluent B; 20–25 min, 40–60% eluent B; 25–30 min, 100% eluent B.

5.2. Synthesis of pyrazolyl-diamine ligand (L1) functionalized with an alendronate unit at the 4-position of the azolyl ring

5.2.1. 2,3,5,6-Tetrafluorophenyl-2-(1-(2-(*tert*-butoxycarbonyl-(2-(*tert*-butoxycarbonyl-amino)ethyl)amino)ethyl)-3,5-dimethyl-1H-pyrazol-4-yl)acetate (II)

To a solution of 2-(1-(2-(*tert*-butoxycarbonyl(2-(*tert*-butoxycarbonylamino)ethyl)amino)ethyl)-3,5-dimethyl-1H-pyrazol-4-yl)acetic acid (I) [14] (577 mg, 1.31 mmol) in dry CH₂Cl₂ and TFF (430 mg, 2.60 mmol) was added dropwise, at 0 °C, a solution of EDC (546 mg, 2.85 mmol) in dry CH₂Cl₂. The reaction mixture was stirred overnight, at room temperature. The solvent was removed under vacuum and the crude was washed with water, giving II (quantitative yield) as a yellow oil.

¹H NMR (CDCl₃, δ): 1.37 (9H, s, 3CH₃); 1.42 (9H, s, 3CH₃); 2.17 (3H, s, CH₃-pz); 2.20 (3H, s, CH₃-pz); 3.11 (2H, t, CH₂); 3.37 (2H, t, CH₂); 3.51 (2H, t, CH₂); 3.66 (2H, s, CH₂); 4.09 (2H, m, CH₂).

5.2.2. 4-(2-(1-(2-(*tert*-butoxycarbonyl(2-(*tert*-butoxycarbonylamino)ethyl)amino)ethyl)-3,5-dimethyl-1H-pyrazol-4-yl)acetamido)-1-hydroxybutane-1,1-diyldiphosphonic acid (III)

To an aqueous solution (3 mL) of alendronate (85 mg, 0.181 mmol) was added NEt₃ to adjust the pH to 10. Compound II (107 mg, 0.181 mmol) was dissolved in dry THF (3 mL) and added dropwise to the solution of alendronate. The reaction mixture was stirred for 5 days at room temperature and the pH maintained at 10. After that time the mixture was purified by a conditioned Sep-Pak C18 (Waters, 12 cc, 2 g) cartridge with a gradient from 100% H₂O to

100% MeOH. Compound III was obtained as a white powder with 58% (49 mg) yield.

¹H NMR (D₂O, δ (ppm)): 1.24 (9H, s, Boc); 1.29 (9H, s, Boc); 1.75–1.83 (4H, m, 2CH₂-ALN); 2.15 (3H, s, CH₃-pz); 2.21 (3H, s, CH₃-pz); 2.65 (2H, t, CH₂); 3.05–3.18 (6H, m, CH₂); 3.50 (2H, br, CH₂), 4.28 (2H, br, CH₂). ³¹P NMR (D₂O, δ): 19.44.

5.2.3. Synthesis of 4-(2-(1-(2-(2-aminoethylamino)ethyl)-3,5-dimethyl-1H-pyrazol-4-yl)acetamido)-1-hydroxybutane-1,1-diyldiphosphonic acid (L1)

TFA (3 mL) was added to compound III (24 mg, 0.036 mmol) and the reaction mixture was stirred for 1 h at room temperature. TFA was removed under vacuum and the crude was purified by washing it with diethyl ether, giving L1 (quantitative) as a white powder.

¹H NMR (D₂O, δ (ppm)): 1.60–1.75 (4H, m, 2CH₂-ALN); 2.09 (3H, s, CH₃-pz); 2.14 (3H, s, CH₃-pz); 3.03 (2H, t, CH₂); 3.20 (2H, br, CH₂); 3.28 (4H, m, CH₂); 3.42 (2H, br, CH₂); 4.44 (2H, br, CH₂). ³¹P NMR (D₂O, δ): 19.56. ¹³C NMR (D₂O, δ): 173.22 (C=O); 112.55 (C-4pz); 147.68 (C-3pz); 143.47 (C-5pz); 73.30 (C); 46.88 (CH₂); 44.92 (CH₂); 44.45 (CH₂); 40.01 (CH₂); 35.54 (CH₂); 31.09 (CH₂); 29.70 (CH₂); 23.40 (CH₂); 9.95 (CH₃); 8.97 (CH₃).

IR (KBr, ν/cm⁻¹): 1670, 1170, 1057. ESI–MS (+) (*m/z*): calc [M + H]⁺, 472.16; found, 472.2. ESI–MS (–) (*m/z*): calc [M – H][–], 470.16; found, 470.2;

5.3. Synthesis of ligands L2 and L3

5.3.1. Synthesis of 4-(2-(3,5-dimethyl-1H-pyrazol-1-yl)ethylamino)-1-hydroxybutane-1,1-diyldiphosphonic acid (V)

The pH of a solution of alendronate (330 mg, 0.85 mmol) and 1-(2-bromoethyl)-3,5-dimethyl-1H-pyrazole (346 mg, 1.70 mmol) in water (3 mL) was adjusted with a 3 M NaOH solution until, approximately, pH = 12. The reaction mixture was refluxed during 48 h and after that time the mixture was purified by a conditioned Sep-Pak C18 (Waters, 12 cc, 2 g) cartridge with a gradient from 100% H₂O to 100% MeOH. Compound V was obtained as a white powder with 32% (107 mg) yield.

¹H NMR (D₂O, δ (ppm)): 1.74 (4H, m, CH₂); 2.03 (3H, s, CH₃-pz); 2.12 (3H, s, CH₃-pz); 2.66 (2H, t, CH₂); 3.02 (2H, t, CH₂); 4.05 (2H, t, CH₂); 5.82 (1H, s, H(4)-pz). ³¹P NMR (D₂O, δ): 18.69. ¹³C NMR (D₂O, δ): 149.4 [C(3/5)pz]; 142.0 [C(3/5)pz]; 105.5 [C(4)pz]; 74.1 (C–OH); 49.2 (CH₂); 47.6 (CH₂); 45.9 (CH₂); 31.7 (CH₂); 23.1 (CH₂); 12.3 (CH₃); 10.2 (CH₃). ESI–MS (+) (*m/z*): calc [M + 3Na – 2H]⁺, 438.2; found, 438.1. ESI–MS (–) (*m/z*): calc [M – H][–], 370.2; found, 370.0; calc [M – 2H + Na][–], 392.2; found, 392.1.

5.3.2. 4-(Bis(2-(3,5-dimethyl-1H-pyrazol-1-yl)ethyl)amino)-1-hydroxybutane-1,1-diyldiphosphonic acid (L2)

Alendronate (330 mg, 0.85 mmol) and compound IV (1.0 g, 5.0 mmol) were dissolved in a water/THF solution (3/1, 8 mL). The pH of the solution was adjusted to 12 with a solution of NaOH 3 M and the reaction mixture was refluxed during 4 days. After this time the mixture was purified by a conditioned Sep-Pak C18 (Waters, 12 cc, 2 g) cartridge with a gradient from 100% H₂O to 100% MeOH. Compound L2 was obtained as a white powder with 60% yield.

¹H NMR (D₂O, δ (ppm)): 1.72 (4H, m, CH₂); 2.03 (6H, s, CH₃-pz); 2.10 (6H, s, CH₃-pz); 2.54 (2H, t, CH₂); 2.78 (4H, t, CH₂); 3.95 (4H, t, CH₂); 5.78 (1H, s, H(4)pz). ³¹P NMR (D₂O, δ): 18.70. ¹³C NMR (D₂O, δ): 149.0 [C(3/5)pz]; 141.7 [C(3/5)pz]; 105.2 [C(4)pz]; 74.2 (C–OH); 54.5 (CH₂); 52.7 (CH₂); 45.4 (CH₂); 32.0 (CH₂); 20.9 (CH₂); 12.2 (CH₃); 10.3 (CH₃). IR (KBr, ν/cm⁻¹): 1676, 1551, 1177, 1119, 1055. ESI–MS (+) (*m/z*): calc [M + 2Na – H]⁺, 538.4; found, 538.3. ESI–MS (–) (*m/z*): calc [M – H][–], 493.4; found, 492.2; calc [M – 2H + Na][–], 514.4; found, 514.1.

5.3.3. Synthesis of 2-((2-(3,5-dimethyl-1H-pyrazol-1-yl)ethyl)(4-hydroxy-4,4-diphosphonobutyl)amino)acetic acid (**L3**)

To a solution of compound V (60 mg, 0.16 mmol) in water (2 mL) was added bromoacetic acid (27 mg, 0.19 mmol). The pH was adjusted to approximately 12 with a solution of NaOH 3 M and the reaction mixture was refluxed overnight. After this time the mixture was purified by a conditioned Sep-Pak C18 (Waters, 12 cc, 2 g) cartridge with a gradient from 100% H₂O to 100% MeOH. Compound L3 was obtained as a white powder with 70% (42 mg) yield.

¹H NMR (D₂O, δ (ppm)): 1.72 (4H, m, CH₂); 2.00 (3H, s, CH₃-pz); 2.10 (3H, s, CH₃-pz); 2.72 (2H, t, CH₂); 3.04 (2H, t, CH₂); 3.21 (2H, s, CH₂); 4.08 (2H, s, CH₂); 5.79 (1H, s, H(4)-pz). ³¹P NMR (D₂O, δ): 18.69. ¹³C NMR (D₂O, δ): 177.8 (C=O); 149.1 [C(3/5)pz]; 141.7 [C(3/5)pz]; 105.5 [C(4)pz]; 74.0 (COH); 57.3 (CH₂); 55.2 (CH₂); 53.1 (CH₂); 45.3 (CH₂); 31.8 (CH₂); 21.2 (CH₂); 12.2 (CH₃); 10.2 (CH₃). IR (KBr, ν/cm⁻¹): 11345, 1261, 1685. Retention time (RP-HPLC): 15.0 min. ESI-MS (+) (m/z): calcd [M + H]⁺, 518.2; found, 518.0. ESI-MS (-) (m/z): calcd [M - H]⁻, 428.3; found, 428.8; calcd [M - 3H + 2Na]⁻, 472.2; found, 472.1.

5.4. General procedure for the synthesis of the Re complexes (**Re3**–**Re5**)

fac-[Re(H₂O)₃(CO)₃]Br was reacted with equimolar amounts of L1–L3 in refluxing water/methanol (L1) or D₂O. The pH was previously adjusted to 6–7 (L1 and L2) or 4 (L3). After 18 h reaction time, the reaction mixtures were cooled to room temperature and the solvent removed under vacuum. The desired complexes were obtained in a pure form after purification with Sep-Pak C18 cartridges (Waters, 12 cc, 2 g) using MeOH/H₂O as eluent and a gradient of 100/0, 25/75, 50/50, 100/0. The pure compounds were lyophilized and obtained as white powders.

5.4.1. fac-[Re(CO)₃(κ³L₁)] (**Re3**)

Re3 (11 mg, 55%) was obtained as a white powder after purification and lyophilization. ¹H NMR (D₂O, δ (ppm)): 1.67–1.85 (4H, m, 2CH₂-ALN); 2.14 (3H, s, CH₃-pz); 2.25 (3H, s, CH₃-pz); 2.77–2.81 (2H, m, CH₂); 3.10 (2H, m, CH₂-ALN); 3.33 (2H, s, CH₂); 3.40–3.55 (4H, m, 4CH₂); 3.64 (1H, m, NH); 3.98–4.07 (2H, m, CH₂); 4.33–4.43 (2H, m, CH₂); 4.96 (1H, br, NH); 6.50 (1H, br, NH). ¹³C NMR (D₂O, δ): 200.66; 180.41 (C=O); 159.04 [C(3/5)pz]; 149.78 [C(3/5)pz]; 118.83 [C(4)pz]; 80.11; 61.37 (CH₂); 55.71 (CH₂); 54.50 (CH₂); 49.68 (CH₂); 48.55 (CH₂); 46.89 (CH₂); 37.88 (CH₂); 37.21 (CH₂); 20.45 (CH₃pz), 16.47 (CH₃pz). ³¹P NMR (D₂O, δ): 19.04. IR (KBr, ν/cm⁻¹): 1666 (C=ONH), 1905, 2025 (CO). Retention time (RP-HPLC): 9.87 min. ESI-MS (-) (m/z): calcd [M + H]⁺, 740.09; found, 740.10.

5.4.2. fac-[Re(CO)₃(κ₃L₂)] (**Re4**)

Re4 (2.0 mg, 13%) was obtained as a white powder after purification and lyophilization. The pH was previously adjusted to 7.0 with DCl and KOD and the reaction mixture heated at 80 °C overnight. ¹H NMR (CD₃OD, δ (ppm)): 1.97 (4H, m, 2CH₂-ALN); 2.05 (6H, s, CH₃-pz); 2.14 (6H, s, CH₃-pz); 3.06 (2H, m, CH₂-ALN); 3.29 (2H, m, CH₂); 3.58 (2+2H, m, 4 HC-H); 4.38 (2H, m, CH₂); 5.95 (2H, s, H(4)-pz). ¹³C NMR (CD₃OD, δ): 199.2; 198.5 (C≡O); 149.4 [C(3/5)pz]; 141.8 [C(3/5)pz]; 105.0 [C(4)pz]; 54.4(CH₂); 52.5 (CH₂); 43.7 (CH₂); 32.6 (CH₂); 20.0 (CH₂); 12.3 (CH₃); 10.3 (CH₃). ³¹P NMR (CD₃OD, δ): 23.03. IR (KBr, ν/cm⁻¹): 1820, 2020 (CO). Retention time (RP-HPLC): 15.5 min. ESI-MS (+) (m/z): calcd [M + H]⁺, 765.1; found, 765.3. ESI-MS (-) (m/z): calcd [M - H]⁻, 763.1; found, 763.2.

5.4.3. fac-[Re(CO)₃(κ₃L₃)] (**Re5**)

Re5 (3.0 mg, 27%) was obtained as a white powder after purification and lyophilization. The pH was adjusted to 4 with DCl and

the reaction mixture was heated at 80 °C overnight. ¹H NMR (D₂O, δ (ppm)): 1.80 (4H, m, 2CH₂-ALN); 2.13 (3H, s, CH₃-pz); 2.29 (3H, s, CH₃-pz); 2.5–2.3 (1H, m, CH); 3.06–3.3 (2+2H, m, CH₂+2 HC-H); 3.78–3.73 (1H, m, CH); 4.20 (2H, m, CH₂); 5.99 (1H, s, H(4)-pz). ³¹P NMR (D₂O, δ): 18.32. IR (KBr, ν/cm⁻¹): 1891, 2026 (CO), 1617 (C=O). Retention time (RP-HPLC): 10.6 min. ESI-MS (+) (m/z): calcd [M + 3Na-2H]⁺, 766.5; found, 766.1; ESI-MS (-) (m/z): calcd [M - H]⁻, 698.0; found, 698.1; calcd [M + Na-H]⁻, 720.0; found, 720.1.

5.5. General procedure for the synthesis of fac-[^{99m}Tc(CO)₃(κ³-L)] (L = L1–L3): Tc3–Tc5

In a nitrogen-purged glass vial, 100 μL of a 10⁻⁴ M (**Tc3**) or 10⁻³ M (**Tc4**, **Tc5**) aqueous solution of the appropriate **L1**–**L3** was added to 900 μL of a solution of the organometallic precursor fac-[^{99m}Tc(CO)₃(H₂O)₃]⁺ (10–18 mCi) in saline at pH 7.4 (**Tc3**, **Tc4**) or at pH 4 (**Tc5**). The reaction mixture was then heated to 100 °C for 30–45 min, cooled on an ice bath and then analyzed by RP-HPLC: R_t = 10.0 min (**Tc3**); R_t = 15.7 min (**Tc4**); R_t = 10.6 min (**Tc5**). The radioactive complexes were obtained with high yield (>95%) and high radiochemical purity (>95%).

5.6. In vitro studies

5.6.1. Lipophilicity

The lipophilicity of the radioconjugate was evaluated by the “shakeflask” method [22]. Briefly, 25 μL of the radioconjugates were added to a mixture of octanol (1 mL) and 0.1 M PBS pH = 7.4 (1 mL), previously saturated in each other by stirring the mixture. This mixture was vortexed and centrifuged (3000 rpm, 10 min, room temperature) to allow phase separation. Aliquots of 25 μL of both octanol and PBS were counted in a gamma counter. The partition coefficient (P_{o/w}) was calculated by dividing the counts in the octanol phase by those in the buffer, and the results expressed as Log P_{o/w}. Log P_{o/w} = -2.08 ± 0.02 (**Tc3**); Log P_{o/w} = -0.97 ± 0.02 (**Tc4**); Log P_{o/w} = -2.18 ± 0.02 (**Tc5**).

5.6.2. Blood serum stability

Complexes **Tc3**–**Tc5** (50 μL) were added to 500 μL of human blood serum and incubated at 37 °C. After incubation (0, 1, 2 and 4 h), aliquots (50 μL) were taken and the proteins precipitated with ethanol (100 μL). The mixture was centrifuged at 3000 rpm for 15 min at 4 °C and the supernatant (protein-free) filtered through a Millipore filter (0.22 μm), and was analyzed by RP-HPLC.

5.6.3. Hydroxyapatite (HA) binding

Adsorption of **Tc3**–**Tc5** onto HA was accomplished following an adaptation of previously described methods [23–25]. Briefly, 50 μL of each complex (~27.8 μCi/25 μL) were incubated for 0, 1, 2 and 4 h at 37 °C in a water bath with 15 mg of solid HA and 500 μL of phosphate-buffered saline (PBS) solution (pH 7.2). The liquid and solid phases were separated by centrifugation (7500 rpm/3 min) and the solid phase washed twice with 500 μL of PBS solution (pH 7.2). The activity in the liquid and solid phases was determined using an ionization chamber.

5.7. Biodistribution studies

The ex-vivo biodistribution of the complexes was evaluated in groups of 4–5 adult Balb/c female mice (Charles River) weighing approximately 15 g each. The animals were injected intravenously with 100 μL (10–32 MBq) of each preparation via the tail vein and were maintained on normal diet ad libitum. All animal studies were conducted in accordance with the highest standards of care, as

outlined in European law. Mice were killed by cervical dislocation at 1 and 4 h after injection. The injected radioactive dose and the radioactivity remaining in the animal at sacrifice were measured with a dose calibrator (Capintec, CRC25R). The difference between the radioactivity in the injected and the sacrificed animal was assumed to be due to total excretion from whole animal body. Blood samples were taken by cardiac puncture when the animals were killed. Tissue samples of the main organs were removed, weighed and counted using a gamma counter (Berthold, LB211). Biodistribution results were expressed as the percentage of the injected activity (I.A.) per gram of tissue. Statistical analysis of the biodistribution data was done by an analysis of variance with GraphPad Prism. Student *t* test was then used to analyze data from each compound versus the reference compound ^{99m}Tc -MDP. The level of significance was set at 0.05.

5.8. *In vivo stability*

The stability of the complexes was assessed in urine and murine serum by RP-HPLC analysis under identical conditions to those used for analyzing the original radiolabelled complexes. The samples were taken 1 h post injection. The urine collected at the sacrifice time was filtered through a Millex GV filter (0.22 μm) before RP-HPLC analysis. Blood collected from the mice was centrifuged at 3000 rpm for 15 min at 4 °C and the serum was separated. The serum was treated with ethanol in a 1:2 (v/v) ratio to precipitate the proteins. After centrifugation at 3000 rpm for 15 min at 4 °C, the supernatant was collected, filtered through a Millex GV filter (0.22 μm) and analyzed by RP-HPLC.

5.9. Cellular uptake

5.9.1. Compounds uptake and distribution

The MDAMB231 breast cancer line was purchased from ATCC (American Type Culture Collection). The cellular uptake experiments were performed with the MDAMB231 cells seeded at a density of 2.5×10^5 cells/500 μL in 24-well plates and allowed to attach overnight. The cells were incubated at 37 °C for 0.5 h–24 h with 5×10^5 – 6×10^5 cpm of the radiolabelled compounds in 0.5 mL DMEM. Incubation was ended by washing the cells with ice-cold medium followed by a two wash steps with cold PBS. Subsequently, the cells were lysed by a 10 min incubation with 1 M NaOH at 37 °C to evaluate the cellular associated radioactivity, at different time points over a 24 h incubation period. The radioactivity in the medium and in the cells were separately collected and counted in a γ -counter. Cellular uptake data was based on three determinations for each time point. and are expressed as mean \pm SD.

For the cellular fractionation experiments MDAMB231 cells (approx. 1×10^6 cells/5 mL medium) were exposed to the radiolabelled bisphosphonates for 6 h at 37 °C, then washed with ice-cold PBS, detached with trypsin solution and centrifuged to obtain a cellular pellet. The cytosol, membrane/particulate,

cytoskeletal and nuclear fractions were extracted using a FractionPREP™, cell fractionation system (BioVision, USA) and performed according to the manufacturer's protocol. The radioactivity of each fraction was counted in a γ -counter.

Acknowledgments

This work has been supported by the Fundação para a Ciência e Tecnologia (FCT) through the project PTDC/QUI-QUI/115712/2009. Sofia Monteiro thanks FCT for a BI research grant. Dr. Joaquim Marçalo is acknowledged for the ESI–MS analyses, which were run on a QITMS instrument acquired with the support of the Programa Nacional de Reequipamento Científico (Contract REDE/1503/REM/2005-ITN) of FCT and as part of RNEM – Rede Nacional de Espectrometria de Massa.

References

- [1] M.G.E.H. Lam, J.M.H.d. Klerk, P.P.v. Rijk, B.A. Zonnenberg, *Anticancer Agents Med. Chem.* 7 (2007) 381–397.
- [2] D.J. Hillegonds, S. Franklin, D.K. Shelton, S. Vijayakumar, V. Vijayakumar, *J. Natl. Med. Assoc.* 99 (2007) 785–794.
- [3] S. Zhang, G. Gangal, H. Uludag, *Chem. Soc. Rev.* 36 (2007) 507–531.
- [4] E. Palma, J.D.G. Correia, M.P.C. Campello, I. Santos, *Mol. BioSystems* 7 (2011) 2950–2966.
- [5] M. Winter, I. Holenb, R.E. Coleman, *Cancer Treat. Rev.* 34 (2008) 453–475.
- [6] S. Senaratne, G. Pirianov, J.L. Mansi, T.R. Arnett, K.W. Colston, *Br. J. Cancer* 82 (2000) 1459–1468.
- [7] C. Denoyelle, L. Hong, J.-P. Vannier, J. Soria, C. Soria, *Br. J. Cancer* 88 (2003) 1631–1640.
- [8] S. Boissier, M. Ferreras, O. Peyruchaud, *Cancer Res.* 60 (2000) 2949–2954.
- [9] S. Boissier, S. Magnetto, L. Frappart, *Cancer Res.* 57 (1997) 3890–3894.
- [10] S. Senaratne, J. Mansi, K. Colston, *Br. J. Cancer* 86 (2002) 1479–1486.
- [11] A.U. Ural, F. Avcu, M. Candir, M. Guden, M.A. Ozcan, *Breast Cancer Res.* 8 (2006) R52.
- [12] S. Alves, A. Paulo, J.D.G. Correia, L. Gano, C.J. Smith, T.J. Hoffman, I. Santos, *Bioconjug. Chem.* 16 (2005) 438–449.
- [13] C. Fernandes, I.C. Santos, I. Santos, H.-J. Pietzsch, J.-U. Kunstler, W. Kraus, A. Rey, N. Margaritis, A. Bourkoula, A. Chiotellis, M. Paravatou-Petsotas, I. Pirmettis, *Dalton Trans.* (2008) 3215–3225.
- [14] C. Moura, T. Esteves, L. Gano, P.D. Raposinho, A. Paulo, I. Santos, *N. J. Chem.* 34 (2010) 2564–2578.
- [15] E. Palma, J.D.G. Correia, B.L. Oliveira, L. Gano, I.C. Santos, I. Santos, *Dalton Trans.* 40 (2011) 2787–2796.
- [16] E. Palma, B.L. Oliveira, J.D.G. Correia, L. Gano, L. Maria, I.C. Santos, I. Santos, *J. Bio. Inorg. Chem.* 12 (2007) 667–679.
- [17] G.R. Kieczkowski, R.B. Jobson, D.G. Melillo, D.F. Reinhold, V.J. Grenda, I. Shinkai, *J. Org. Chem.* 60 (1995) 8310–8312.
- [18] P. López, C.G. Seipelt, P. Merklung, L. Sturz, J. Álvarez, A. Dölle, M.D. Zeidler, S. Cerdán, P. Ballesteros, *Bioorg. Med. Chem.* 7 (1999) 517–527.
- [19] P. Mougenot, P. Mertens, M. Nguyen, R. Touillaux, J. Marchand-Brynaert, *J. Org. Chem.* 61 (1996) 408–412.
- [20] <http://www.cyberlipid.org/phlipt/pl2a0006.htm>, 2013-09-15.
- [21] N. Lazarova, S. James, J. Babich, J. Zubietta, *Inorg. Chem. Commun.* 7 (2004) 1023–1026.
- [22] T.J. Hoffman, W.A. Volkert, D.E. Troutner, R.A. Holmes, *Int. J. Appl. Radiat. Isot.* 35 (1984) 223–225.
- [23] M. Försterová, Z. Jandurová, F. Marques, L. Gano, P. Lubal, J. Vaněk, P. Hermann, I. Santos, *J. Inorg. Biochem.* 102 (2008) 1531–1540.
- [24] W.P. Li, D.S. Ma, C. Higginbotham, T. Hoffman, A.R. Ketring, C.S. Cutler, S.S. Jurisson, *Nucl. Med. Biol.* 28 (2001) 145–154.
- [25] F. Marques, L. Gano, M. Paula Campello, S. Lacerda, I. Santos, L.M.P. Lima, J. Costa, P. Antunes, R. Delgado, *J. Inorg. Biochem.* 100 (2006) 270–280.